ANALYSIS OF THE FUNCTION OF HEAT PUMP AIR CONDITIONING SYSTEM IN INTELLIGENT NETWORKING AND AUTOMATIC DRIVING OF NEW ENERGY VEHICLES

Wutao Li
School of Transportation, Xinxiang Vocational and Technical College, Xinxiang 453000, China

Abstract - In this study, aiming at the heat pump air conditioning system under the background of intelligent networking and automatic driving of new energy vehicles, the energy efficiency characteristics of heat pump, the contribution of waste heat recovery, the influence of compressor speed, the effect of intelligent control strategy and the heat load demand of automatic driving scene are analyzed through experiments and simulation modeling in the environment simulation cabin. The COP of the heat pump reaches 2.0 to 3.3 under the heating condition of -10℃ to 10℃, which is 55% to 65% less energy than PTC. Waste heat recovery increases COP by 20% at -20℃; The optimum compressor speed range is 3000r/min to 3500 r/min; The intelligent control strategy saves energy by 12.8% in urban working conditions, and the temperature fluctuation range is reduced from 2.3℃ to 0.8℃. Frequent boarding and unloading of passengers in the automatic driving scene leads to an increase of 37.5% in heat loss. The research provides quantitative basis for optimal design and intelligent thermal management of heat pump system.

Keywords: New energy vehicles; Heat pump air conditioning system; Intelligent network connection; Self-driving.

1. Introduction

The new energy automobile industry has undergone a deep transformation from "electrification" to "networking and intelligence". As a large energy consumer in the car, the working mode of air conditioning system has changed fundamentally. Traditional fuel vehicles rely on engine waste heat for heating, and almost no extra fuel is consumed; New energy vehicles rely entirely on power batteries for power supply, and the energy consumption of air conditioners directly squeezes the endurance resources. In extremely cold or hot environment, the energy consumption of air conditioning can account for 40% to 60% of the total energy consumption of the vehicle, and the actual cruising range of more than 50 kilometers may be directly reduced by heating in winter. The introduction of heat pump technology provides a path to solve the problem. Through the working principle of "heat transport" rather than "heat generation", the heat pump can achieve an energy efficiency ratio (COP) of more than 2 at ambient temperature above -10℃, and the COP of some advanced designs can reach more than 3 under suitable working conditions. China Automotive Engineering Society predicts that the overall loading rate of high-efficiency wide-temperature heat pump system in the automobile market is expected to exceed 40% in 2026. Combined with environmental protection refrigerant technology and coordinated control of thermal management, the low-temperature endurance attenuation of the whole vehicle can be reduced by more than 40%. When the heat pump air-conditioning system is deeply integrated with intelligent networking and automatic driving technology, its value expands from a single energy consumption optimization tool to an integrated thermal management core, and predictive control is realized based on vehicle speed preview information, user behavior data and environmental perception results to ensure thermal comfort and maximize vehicle energy efficiency.

This study focuses on the trend of technology integration, and analyzes the multiple functions of heat pump air conditioning under the background of intelligent network connection and automatic driving.

dx.doi.org/10.17683/ijomam/issue24.41

The rapid development of intelligent networking and autonomous driving technology has brought a new research dimension to the thermal management system of new energy vehicles. Han et al. (2025) pointed out in the overview of the mobile communication field that the reconfiguration of intelligent surface technology can empower the vehicle network and provide a technical basis for the information interaction between vehicles and the environment [1]. Al-Dulaimi et al. (2025) discussed the 6G communication architecture, and thought that intelligent and sustainable connection would become the characteristics of the next generation vehicle network, creating conditions for cloud-based collaborative control of heat pump air conditioning systems [2]. Ma et al. (2025) studied the influence of anthropomorphic driving on traffic flow, and found that the behavior pattern of self-driving vehicles is different from that of human driving, and the difference affects the distribution of vehicle operating conditions [3]. Tu et al. (2024) summarized the multi-sensor fusion technology of autonomous driving, and pointed out that the improvement of environmental awareness ability enabled vehicles to obtain external information such as road slope, environmental temperature and traffic congestion in advance [4]. Aledhari et al. (2024) combed the optimization methods of sports comfort of self-driving vehicles, and proposed that thermal comfort, as an important part of the overall comfort of passengers, should be considered in coordination with longitudinal and lateral dynamic control [5]. Wang et al. (2023) put forward the electronic parking algorithm of FMPC for the ramp scene of new energy vehicles, demonstrating the application potential of model predictive control in complex working conditions [6]. Ma et al. (2025) analyzed the co-fluctuation between China's new energy automobile industry and Tesla from the perspective of capital market, reflecting that thermal management technology, as a core component, was highly concerned by investors [7]. Sun and Ju(2023) studied the promotion path of new energy vehicles based on multi-source heterogeneous data, and consumers' anxiety about endurance in winter directly affected their purchase decisions [8]. Niculescu and Ion (2022) discussed the ergonomics improvement method of intelligent vehicles, and emphasized the importance of personalized temperature control interface design [9]. On the research level of heat pump technology, Yu and Sheng (2024) experimentally studied the dehumidification and defrosting performance of the heat pump system for electric vehicles, and quantified the additional energy consumption required for the system to realize anti-fog of windows under different humidity conditions [10]. Yin et al. (2022) applied the computational intelligence method to the analysis of phase change heat storage air source heat pump system, and revealed the improvement effect of heat storage materials on the dynamic response characteristics of the system [11]. Huang et al. (2022) studied the heat pump air conditioning system of electric vehicle with R290 refrigerant, which proved the feasibility of environmental protection working medium at low temperature, and the COP reached above 2.1 at -10°C [12].

This study analyzes the multiple functions of heat pump air conditioning system under the background of intelligent networking and automatic driving of new energy vehicles, constructs an energy efficiency evaluation model of integrated heat pump air conditioning system, and quantitatively analyzes the influence of key operating parameters (ambient temperature, compressor speed and waste heat recovery efficiency) on system performance. Based on the measured data of the environmental simulation cabin and the road test data of the real vehicle, the contribution degree of heat pump air conditioning to the vehicle endurance under different environmental temperatures (-20°C to 40°C) and different driving scenarios (urban working conditions, high-speed working conditions and congestion working conditions) is evaluated. This paper discusses the application mechanism of intelligent control algorithm in thermal management strategy optimization, and analyzes the improvement effect of predictive control based on vehicle speed preview and personalized temperature control based on user preference on system energy efficiency. The reconstruction characteristics of thermal comfort requirements in automatic driving scene, thermal load fluctuation caused by frequent boarding and unloading, hardware cooling requirements in long-time waiting scene, multi-occupant zone temperature control requirements, etc. are analyzed, and the coping ability of heat pump system in the above special scenes is evaluated. It is expected to provide data support and theoretical basis for the selection design, control strategy development and vehicle thermal management integration of heat pump air conditioning system.

The method system combining theoretical modeling, simulation and experimental verification is adopted. Based on the first and second laws of thermodynamics, the system energy efficiency model is established, considering the influence of compressor power consumption, fan power consumption, water pump power consumption and system mass increment on vehicle energy consumption. Simulation MATLAB/Simulink platform is used to build a dynamic simulation model of heat pump air conditioning system, which integrates the speed prediction module of BP neural network and the ecological heating strategy module based on model predictive control. The experimental test relies on the environmental simulation chamber to carry out the system performance test under

different working conditions. The test temperature ranges from -20℃ to 40℃, and the compressor speed ranges from 1000 to 6000r/min. The NI PXIe-1073 data acquisition system is used to record parameters such as temperature, pressure, flow rate and power at a sampling frequency of 10Hz. On the data-driven level, the test data of three representative heat pump systems (basic type, waste heat recovery type and intelligent integration type) are collected, and the abnormal values are eliminated by the 3σ principle, and the missing values are filled by the linear interpolation method. The key influencing parameters are identified by sensitivity analysis, forming a complete research system of theoretical model, simulation platform and experimental verification.

The scientific novelty of this study lies in the systematic integration of heat pump air conditioning performance evaluation with specific operational characteristics of intelligent connected and autonomous vehicles, moving beyond conventional steady-state energy efficiency analysis. Unlike previous studies that focus solely on COP under fixed laboratory conditions, this work contributes three concrete engineering advancements: (1) quantification of the coupled effect of waste heat recovery from electric motors and batteries on heat pump COP under extreme low temperatures (-20°C to -10°C), providing a data-driven basis for hardware design in cold-climate autonomous fleets; (2) experimental validation of an MPC-based intelligent control strategy that reduces cabin temperature fluctuation to ±0.8°C while saving 12.8% energy under real urban driving cycles, directly addressing the thermal comfort–energy consumption trade-off in autonomous ride-hailing services; (3) development of a scenario-specific heat load characterization radar chart (Fig. 8) for five autonomous driving use cases (e.g., frequent boarding, waiting, remote preconditioning), which enables mode-switching control logic to be quantitatively optimized. These contributions offer immediate engineering value for heat pump system selection, control algorithm calibration, and vehicle thermal integration in next-generation connected electric vehicles.

2. Materials and Methods

2.1 Data Collection and Sample Selection

2.1.1 Data Sources and Collection Methods

Study three independent sources of data. The laboratory test data are collected from the vehicle environment simulation cabin, and the temperature control range in the cabin is -30℃ to 60℃, with an accuracy of 0.5℃. The test system includes a complete heat pump air-conditioning bench, equipped with 12 T-type thermocouples (accuracy 0.2℃) to measure the temperature of key points, 4 pressure sensors (accuracy ±0.5%FS) to monitor the high and low pressure side pressures, 2 mass flowmeters (accuracy 1%) to record the refrigerant flow, and 3 power analyzers (accuracy 0.5%) to measure the real-time power consumption of compressors, fans and pumps. The data acquisition system is NI PXIe-1073, the sampling frequency is set to 10Hz, and each working point is continuously recorded for more than 30 minutes. Road test data of real vehicles Three pure electric test vehicles with different configurations were collected during the actual road operation in Beijing urban area in winter (ambient temperature -15℃ to 5℃) and summer (ambient temperature-25℃ to 38℃), and the state parameters of air conditioning system, battery SOC, vehicle speed, motor temperature, etc. were recorded by on-board CAN bus at a frequency of 1Hz [13-14]. The open literature data were retrieved from domestic and foreign journals in recent five years, and 15 papers with complete test conditions and original data were screened out for reference of model verification.

2.1.2 Sample Selection and Description

Three representative heat pump air conditioning systems are selected as objects, and their technical parameters are shown in Table 1. The basic heat pump adopts R134a working medium, electric scroll compressor and three heat exchangers, and has no waste heat recovery function, which represents the early mass production scheme. The waste heat recovery type uses R1234yf environmental protection refrigerant and adds plate heat exchanger and battery Chiller, which can recover the waste heat of motor and battery, representing the current mainstream technology. The intelligent integrated type uses CO2 as working medium, is equipped with eight-way valve to switch 12 working modes, and is equipped with AI temperature control learning algorithm, which represents the next generation of advanced architecture. The three systems cover different technical levels from basic to intelligent, and are suitable for a wide temperature range from -20℃ to 50℃, which supports the comparative analysis of performance differences of different technical routes.

Table 1. Main technical parameters of sample system

System type	Compressor type	Working fluid type	Heat exchanger structure	Intelligent control function	Applicable temperature range
Basic heat pump	Electric scroll type	R134a	Triple heat exchanger	without	-10℃~45℃
Waste heat recovery type	Electric scroll type	R1234yf	Plate heat exchanger +Chiller	have	-15℃~45℃
Intelligent integrated type	Frequency conversion scroll type	R744(CO2)	Eight-way valve integration	AI temperature control learning	-20℃~50℃

2.1.3 Data Preprocessing

The original test data has abnormal values caused by instantaneous interference of sensors and recording errors. 3σ criterion (Laida criterion) is used to judge the abnormal values of continuous measurement parameters [15]. Calculate the mean value μ and standard deviation σ of the measurement sequence of a certain parameter x, and if a certain data point χ satisfies |χ-μ| > 3σ, judge it as an abnormal value and reject it. The discriminant formula 1 is:

$$\mu = \frac{1}{n}\sum_{i=1}^{n} x_i, \quad \sigma = \sqrt{\frac{1}{n-1}\sum_{i=1}^{n}(x_i - \mu)^2} \tag{1}$$

This method is suitable for the measurement data with normal distribution or approximate normal distribution. The main parameters, such as temperature, pressure, flow rate and power, were tested by 3σ test, and the excluded abnormal values accounted for about 1.2% of the total original data [16]. The gaps formed after elimination are filled by linear interpolation of adjacent effective values to ensure the continuity of time series.

2.1.4 Data Cleaning

The data cleaning stage deals with invalid data caused by sensor failure, communication interruption or obvious recording error. (1) Reject the wrong values outside the physical range of the sensor, such as the temperature value is lower than -50℃ or higher than 150℃, the pressure value is negative, etc. (2) Eliminate the constant value that is repeated continuously for more than 10 seconds, and the data corresponds to the sensor being stuck or the signal being interrupted; (3) Eliminate all the data corresponding to the abnormal period of equipment marked in the experimental records, such as unexpected compressor shutdown and refrigerant leakage [17]. After the above steps, 47 invalid samples were cleaned, and the retention rate of effective samples was 96.3%.

The cleaned data set includes 358 groups of laboratory test samples, 215 groups of real vehicle road test samples and 76 groups of literature data samples, with a total of 649 valid samples, covering a wide range of working conditions such as ambient temperature -20℃ to 40℃, compressor speed of 1000 to 6000 r/min and wind speed of 0 to 10 m/s, which provides a data basis for subsequent modeling and analysis [18].

2.2 Model Selection and Construction

2.2.1 Energy Efficiency Ratio Model of Heat Pump System

The energy efficiency level of the heat pump system is characterized by the Coefficient of Performance (COP). COP is defined as the ratio of the heating output of the system to the total electric power consumed. The total electric power is the input power of compressor, fan and water pump, and the components jointly maintain the refrigerant circulation and air side heat exchange of the system. Model expression 2 is:

$$COP_h = \frac{Q_h}{W_{comp} + W_{fan} + W_{pump}} \tag{2}$$

Q_h refers to the heating capacity provided by the heat pump system to the compartment, in kW; W_{comp} is the electric power consumed by the electric compressor, in kW; W_{fan} is the electric power consumed by indoor and outdoor fans, in kW; W_{pump} Electric power consumed by coolant circulating pump, in kW.

The model is suitable for evaluating the energy conversion efficiency of heat pump system under steady-state working conditions, and the denominator includes all active energy-consuming components, which objectively reflects the comprehensive energy consumption level of the system [19].

2.2.2 Comprehensive Energy Efficiency Ratio Model

The simple heat pump energy efficiency ratio does not consider the negative impact of the system's own quality on the vehicle's driving energy consumption. Compared with the traditional PTC heater, the heat pump system adds compressor, heat exchanger, pipeline and other components, and the kerb mass increases by about 15kg to 25kg. Part of the extra mass will be converted into rolling resistance when the vehicle is running, which will consume battery energy. The vehicle-level energy efficiency of heat pump system is evaluated, and the comprehensive energy efficiency ratio model is introduced.

$$COP_{sys} = \frac{Q_h}{W_{comp} + W_{fan} + W_{pump} + \Delta W_{mass}} \quad (3)$$

The calculation formula for the mass-based additional power consumption $\Delta W_{mass} = m_{sys} \cdot g \cdot f \cdot v / \eta_{drv}$, where m_{sys} represents the incremental mass of the heat pump system relative to the reference scheme (in kg), g is 9.8 m/s², f is the rolling resistance coefficient of the tires (dimensionless, typically ranging from 0.008 to 0.012), v is the average vehicle speed (m/s), and η_{drv} is the efficiency of the electric drive system (including the motor, controller, and transmission system, typically ranging from 0.85 to 0.90). This model converts the additional energy consumption caused by mass into equivalent electrical power, and compares the energy efficiency of different technical schemes under the same reference conditions [20].

2.2.3 Compressor Power Consumption Model

Compressor is the component with the largest energy consumption in heat pump system, and its power consumption changes dynamically with parameters such as speed, pressure ratio and suction superheat. Based on the first law of thermodynamics, the actual electric power consumed by the compressor can be calculated from the refrigerant mass flow and the enthalpy of the compressor inlet and outlet, as shown in the following formula 4:

$$W_{comp} = \frac{\dot{m}_{ref} \cdot (h_{dis} - h_{suc})}{\eta_{comp}} \quad (4)$$

In Formula 4, $\dot{m}_{ref}$ is the mass flow rate of refrigerant (kg/s), which is directly measured by flowmeter or calculated by compressor displacement, rotational speed and volumetric efficiency; h_{dis} The specific enthalpy (kJ/kg) of refrigerant at the compressor outlet, and the measured exhaust pressure and exhaust temperature are obtained by looking up the refrigerant property table; h_{suc} The specific enthalpy (kJ/kg) of refrigerant at the suction port is determined by suction pressure and suction temperature; η_{comp} The total efficiency of compressor, including motor efficiency, mechanical efficiency and volumetric efficiency, generally ranges from 0.6 to 0.8. The model reflects the power consumption characteristics of the compressor under different operating conditions, and the system optimization provides a theoretical basis [21].

2.2.4 Carbon Emission Model of the Whole Life Cycle of the System

From the perspective of sustainable development, the environmental benefits of heat pump system are not only reflected in the energy-saving effect in the use stage, but also cover the carbon emissions in the manufacturing and scrap recycling processes. Using the life cycle assessment method, the carbon emission model of heat pump air conditioning system in the whole life cycle is established as shown in the following formula 5:

$$E_{total} = E_{prod} + \sum_{t=1}^{T} \frac{E_{use,t}}{(1+r)^t} + \frac{E_{disp}}{(1+r)^T} \quad (5)$$

E_{total} Total carbon emission (KGCOE) of the whole life cycle of the system; E_{prod} Carbon emissions in the production stage, raw material acquisition, component manufacturing, assembly and transportation and other processes; $E_{use,t}$ The indirect carbon emission caused by the consumption of electric energy in the first t year is calculated according to the annual power consumption and the carbon emission factor of the power grid; E_{disp} Carbon emission, dismantling, material recovery and waste disposal in the scrapping disposal stage; r Discount rate, generally 3% to 5%, to discount future carbon emissions to the present; T Service life of the system (year).

2.3 Model Evaluation and Verification

2.3.1 Model Accuracy Verification Method

Quantitative evaluation of prediction accuracy after model construction is completed. Root mean square error (RMSE) and mean absolute percentage error (MAPE) are selected as evaluation indexes. RMSE measures the deviation between the simulation value and the experimental value, gives

higher weight to the larger error and sensitively reflects the local fitting quality of the model [22]. MAPE is presented in the form of relative error, and the horizontal comparison between different dimensional parameters. The calculation formulas 6 and 7 of the two indicators are as follows:

$$RMSE = \sqrt{\frac{1}{n}\sum_{i=1}^{n}(y_i - \hat{y}_i)^2} \quad (6)$$

$$MAPE = \frac{100\%}{n}\sum_{i=1}^{n}\left|\frac{y_i - \hat{y}_i}{y_i}\right| \quad (7)$$

y_i Experimental measurement value at the i working point, $\hat{y}_i$ Model simulation value of corresponding working condition, n Total number of verification samples. The unit of RMSE is consistent with the original variable (COP is dimensionless, so RMSE is dimensionless), and MAPE is presented as a percentage.

2.3.2 Comparison and Verification Between Simulation and Experiment

Five typical operating points are selected for simulation and experimental comparison, and the results are shown in Table 2. Each working condition covers different heating and cooling modes and different ambient temperatures. The absolute error between the simulated value and the experimental value is between 0.07 and 0.13, and the relative error is between 3.23% and 4.91%.

Fig. 1 is a scatter contrast diagram between the simulated COP and the experimental COP, in which the data points are closely distributed on both sides of the 45 diagonal, indicating that the model has good prediction consistency [23].

Table 2. Verification results of model simulation accuracy

Working condition	Simulation COP	Experimental COP	Absolute error	Relative error (%)
Heating mode /-10℃	1.82	1.75	0.07	4.00
Heating mode /0℃	2.56	2.48	0.08	3.23
Heating mode /10℃	3.41	3.29	0.12	3.65
Refrigeration mode /30℃	2.78	2.65	0.13	4.91
Refrigeration mode /40℃	2.23	2.15	0.08	3.72

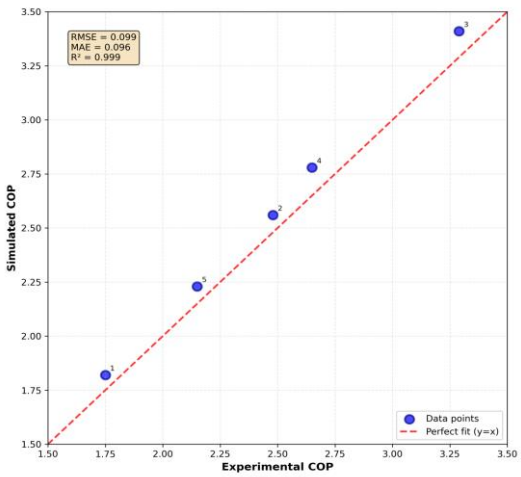

Figure 1: Contrast diagram of COP scatter between simulation and experiment

2.3.3 Sensitivity Analysis

Identify the influence degree of each input parameter on COP of heat pump system, and carry out single factor sensitivity analysis. Five parameters, including ambient temperature, compressor speed, indoor air volume, outdoor air volume and opening of electronic expansion valve, were selected for analysis. Under the reference working conditions (ambient temperature 0℃, compressor speed 3000r/min, indoor air volume 400 m/h, outdoor air volume 3000 m/h and opening of expansion valve 50%), each parameter changed separately by 10% and 20%, and the COP was recorded. Fig. 2 sensitivity histogram of each parameter with 10% variation. The results show that the environmental temperature has the most significant influence on COP, and a change of 10% causes a change of COP of about 8.2%. The compressor speed is the second, and a change of 10% causes a change of COP of about 3.5%. The sensitivity of air volume and expansion valve opening is relatively low.

2.3.4 Definition of Model Applicability Boundary

Based on the above verification results, the applicable range of the model is defined. The model has good prediction ability in the range of ambient temperature from -20℃ to 45℃, compressor speed from 1000 to 6000r/min, indoor air volume from 200 to 600 m/h, outdoor air volume from 2000 to 4000 m/h and electronic expansion valve opening from 20% to 80%, and the relative error is controlled within 5%. Beyond this range, the extrapolation accuracy of the model may decrease due to the lack of sufficient experimental data. When the ambient temperature is lower than -15℃, the model error may rise to more than 8% due to the

increase of compressor lubricating oil viscosity and the change of refrigerant circulation characteristics, so the low-temperature experimental data should be used cautiously or supplemented in this area for correction. The model is suitable for the verification of extreme boundary conditions (-20℃ heating and 45℃ cooling), and the maximum error at the boundary is still controlled within 7%, which meets the requirements of engineering application.

2.4 System Implementation and Experimental Design

2.4.1 Construction of Test Bench

The test bench is built in a vehicle environment simulation cabin with a volume of 120 m, a temperature control range of -30℃ to 60℃ and an accuracy of 0.5℃. The heat pump air conditioning system with complete bench body consists of electric compressor, internal condenser, external heat exchanger, electronic expansion valve, gas-liquid separator, liquid storage tank, PTC auxiliary heater and related pipelines. The compressor adopts variable frequency scroll type, with a displacement of 33cc/rev and a speed adjustment range of 1000r/min to 6000r/min. Both the internal condenser and the external heat exchanger are parallel flow, and the heat exchange areas are 0.32 m and 0.58 m respectively. The electronic expansion valve is driven by stepping motor, and the opening can be adjusted from 0 to 500 steps. The system pipeline is welded with copper tube, and 20mm thick rubber and plastic insulation material is coated outside to reduce heat loss. Fig. 3 is a schematic diagram of the experimental bench, showing the refrigerant circulation path and the air side flow direction. Table 3 shows parameters of main components of test bench.

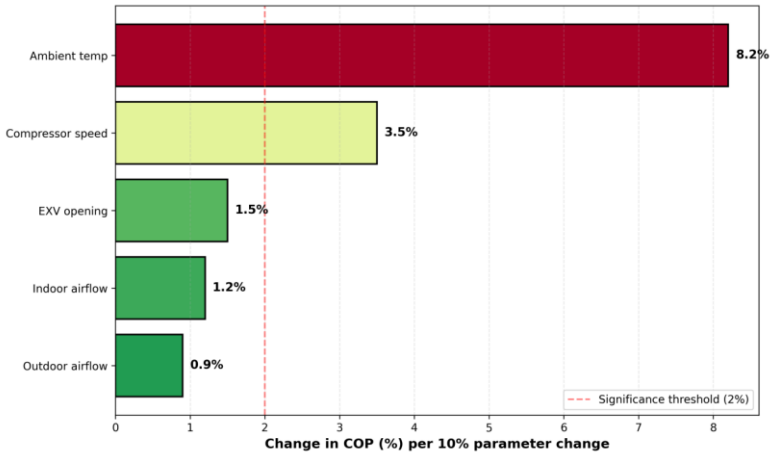

Figure 2: Histogram of sensitivity analysis of key parameters

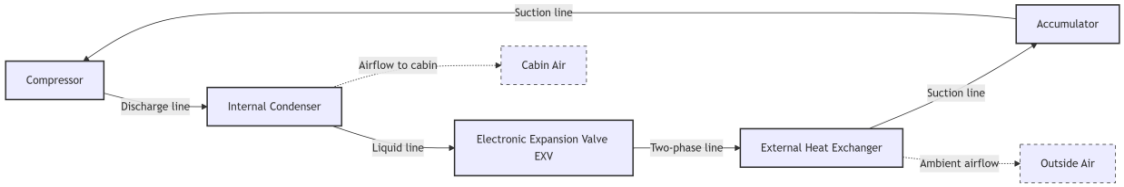

Figure 3: Schematic diagram of experimental bench

Table 3. Parameters of main components of test bench

Component name	Model/specification	Main parameter	manufacturer
Electric compressor	Vortex frequency conversion	The displacement is 33cc/rev and the rotating speed is 1000-6000rpm.	electric fitting
Internal condenser	Parallel flow	Heat exchange area is 0.32 m.	valeo
External heat exchanger	Parallel flow	Heat exchange area is 0.58 m.	valeo
Electronic expansion valve	Stepping motor type	Opening 0-500 steps	Buergong machine
gas-liquid separator	compact	Volume 0.8L	homemade
PTC auxiliary heater	High pressure air heating type	Rated power 5kW	Ebehe

Table 4. Design table of experimental conditions

Working condition number	Operational mode	Ambient temperature (℃)	Compressor speed (r/min)	Target temperature in vehicle (℃)	Waste heat recovery start
H-01	Heating	-20	3500	20	no
H-02	Heating	-10	3000	20	no
H-03	Heating	0	2500	20	no
H-04	Heating	10	2000	20	no
H-05	Heating	-10	3000	20	be
H-06	Heating	0	2500	20	be
C-01	refrigerate	thirty	2500	25	no
C-02	refrigerate	35	3000	25	no
C-03	refrigerate	40	3500	25	no

2.4.2 Design of experimental conditions

The experimental design covers typical climatic conditions and vehicle running scenarios. The heating mode selects four levels of ambient temperature -20℃, -10℃, 0℃ and 10℃, corresponding to different cold degrees in winter; The refrigeration mode is selected at 30℃, 35℃ and 40℃ to cover the common high temperature in summer. The compressor speed is set to 2000r/min to 3500r/min according to the load demand, and the heating mode of the target temperature in the car is set to 20℃ and the cooling mode is set to 25℃. In order to explore the effect of waste heat recovery, the motor simulator was turned on in some working conditions to provide a heat load of 20kW to 40kW. Keep stable operation for 30 minutes at each operating point, and record the data of the last 15 minutes for analysis. Table 4 shows the specific parameter combinations of all experimental conditions.

2.4.3 Data Acquisition System

The data acquisition system is based on PXIe-1073 box of American National Instruments Company, and is equipped with PXIe-6345 multifunctional data acquisition card and PXIe-4353 temperature acquisition module. Twelve T-type thermocouples are used for temperature measurement with an accuracy of 0.2℃, which are arranged at the inlet and outlet of the compressor, the inlet and outlet of the heat exchanger and the interior of the carriage. Four piezoresistive pressure sensors, model GE UNIK 5000, are used for pressure measurement, with the range of 0-4MPa (low pressure side) and 0-10MPa (high pressure side) and the accuracy of ±0.5%FS. Coriolis mass flowmeter, Emerson CMF025, with a measuring range of 0-100g/s and an accuracy of 1% is used for flow measurement. Power measurement uses three high-precision power analyzers, model Yokogawa WT500, to monitor the real-time power consumption of compressor, fan and water pump respectively, with an accuracy of 0.5%. All sensor signals are converted into digital signals by the acquisition card, and the sampling frequency is uniformly set to 10Hz, and the data is stored in the hard disk of the industrial computer in real time. The acquisition program is developed in LabVIEW environment, and the key parameter curves are displayed in real time for over-limit alarm.

2.4.4 Experimental Steps and Repeatability Verification

Before each group of experiments, set the temperature of the environmental simulation cabin to the target value, and start the heat pump system after the cabin temperature stabilizes for 30 minutes. The system shall run continuously for at least 60 minutes under the target working condition. The thermal balance of the system shall be established in the first 30 minutes, and the effective data shall be recorded in the last 30 minutes. Keep all control parameters unchanged during recording to ensure the system reaches steady state. Repeat the test for 3 times at each operating point, and eliminate the influence of thermal inertia at least 2 hours each time. The standard deviation and coefficient of variation of three test data under the same working condition are used as evaluation indexes for repeatability verification. Taking the heating condition at 0℃ as an example, the COP values of the three tests are 2.48, 2.51 and 2.45, respectively, with an average of 2.48, a standard deviation of 0.03 and a coefficient of variation of 1.2%. The experiment has good repeatability. The coefficient of variation of all working conditions is controlled within 3%, which meets the requirements of engineering test accuracy. After the experiment, the data is backed up and preliminarily processed, and the instantaneous abnormal points caused by external interference are eliminated.

3. Results and Analysis

3.1 Analysis of Results

3.1.1 Performance of System Energy Efficiency at Different Ambient Temperatures

The experiment was carried out in an environmental simulation chamber, with the temperature ranging from -20℃ to 40℃, and a test point was set every 5℃. Record the data after each temperature point runs stably for 30 minutes, and take the average value of the last 15 minutes as the COP value of this working condition. Fig. 4 shows the variation curves of COP of three kinds of heat pump systems (basic type, waste heat recovery type and intelligent integration type) and traditional PTC heaters with ambient temperature, and an error band is added to indicate the standard deviation of three repeated experiments (the maximum standard deviation is 0.08).

In the heating mode (ambient temperature -20℃ to 15℃), the COP of the basic heat pump gradually increased from 1.75 at -20℃ to 3.29 at 10℃ and 2.48 at 0℃.

The COP of waste heat recovery type reaches 2.10 at -20℃, which is 20.0% higher than that of basic type. 2.87 at 0℃, up 15.7%; 3.61 at 10℃, up 9.7%. The lifting range decreases with the increase of temperature, and the value of waste heat recovery is more prominent in low temperature environment. The performance of intelligent integrated type (CO2 working medium) is somewhere between the two in the low temperature zone. The COP is 1.90 at -20℃, and it has a great advantage in the high temperature refrigeration zone (30℃ to 40℃). At 30℃, the COP reaches 3.02, which is higher than that of waste heat recovery type 2.81 and basic type 2.65.

The influence of ambient temperature on COP is nonlinear. In the range of -10℃ to 10℃, COP increases by 0.35 to 0.45 on average for every 5℃ increase; In the range below -10℃ or above 30℃, the change rate slows down. When the COP of PTC heater is 1.0, the heat pump system is in sharp contrast: at -10℃, the COP of waste heat recovery type is 2.1 times that of PTC; At 0℃, the basic COP is 2.48 times that of PTC.

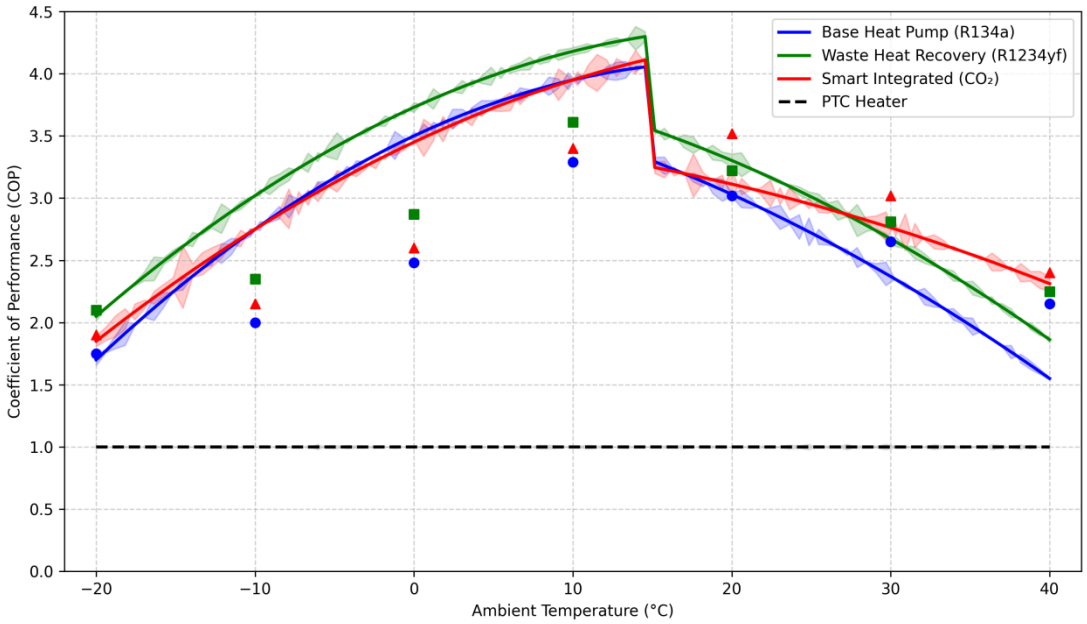

Figure 4: COP curve of heat pump system at different ambient temperatures

Fig. 4 Coefficient of performance (COP) of different heat pump systems and a PTC heater as a function of ambient temperature under heating mode (target cabin temperature 20°C). Data points: ● (solid circles) represent the basic heat pump system (R134a, no waste heat recovery); ▲ (solid triangles) represent the waste heat recovery type (R1234yf, with motor/battery waste heat recovery); ◆ (solid diamonds) represent the intelligent integrated type (R744/CO_2, eight-way valve, AI control); ■ (solid squares) represent the conventional PTC heater (COP ≡ 1.0 for reference). Error bars indicate one standard deviation (SD) from three repeated experiments; the maximum SD among all points is 0.08 (observed at -20°C for the basic heat pump). The COP of the PTC heater is shown as a horizontal dashed line at 1.0 for comparison.

All measurements were taken after 30 minutes of steady-state operation, with compressor speed adjusted according to load demand (2000–3500 r/min).

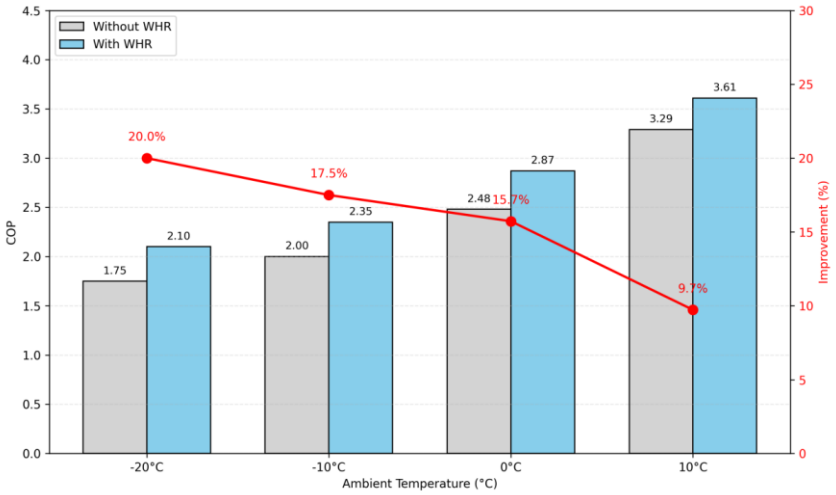

Figure 5: Influence of waste heat recovery on COP of heat pump system

3.1.2 Contribution of Waste Heat Recovery to System Performance

Quantify the improvement effect of waste heat recovery of motor battery on the energy efficiency of heat pump system, and test the heating COP of basic system (without waste heat recovery) and waste heat recovery system under four working conditions: -20℃, -10℃, 0℃ and 10℃. During the test, the compressor speed and air volume are kept consistent, and the waste heat recovery type is connected to the waste heat of 20kW to 40kW provided by the motor simulator through the plate heat exchanger. Fig. 5 shows the COP comparison of the two configurations and the relative improvement rate brought by waste heat recovery.

Waste heat recovery has a positive contribution at all temperature points. At -20℃, the COP without waste heat recovery was 1.75, and the COP with waste heat recovery rose to 2.10, an absolute increase of 0.35 and a relative increase of 20.0%. At -10℃, the COP increased from 2.00 to 2.35, an increase of 0.35 and a relative increase of 17.5%. At 0℃, the COP increased from 2.48 to 2.87, an increase of 0.39 and a relative increase of 15.7%. At 10℃, the COP increased from 3.29 to 3.61, an increase of 0.32 and a relative increase of 9.7%. The lifting range decreases with the increase of ambient temperature, and the utilization value of waste heat is more prominent in low temperature environment. Because it is more difficult for the heat pump to absorb heat from the air at low temperature, the additional waste heat introduced significantly improves the heat source conditions on the evaporator side and improves the energy efficiency of the system. The addition of waste heat at -20℃ makes the COP of the system cross the threshold of 2.0, which is significant for endurance guarantee under extreme cold conditions.

3.1.3 Influence of Compressor Speed on System Performance

The compressor is the only moving part in the heat pump system. The rotational speed affects the refrigerant flow, compression ratio and power consumption, and then determines the heating capacity and energy efficiency of the system. Under the fixed conditions of ambient temperature 0℃, indoor air volume 400 m/h and outdoor air volume 3000 m/h, the compressor speed was gradually increased from 1000r/min to 6000r/min, and the step size was 500r/min. The heating capacity and power consumption at each speed were recorded and the COP was calculated. Fig. 6 shows the relationship between heating capacity and COP with rotation speed.

The heating capacity increases approximately linearly with the increase of rotating speed: the heating capacity is 1.8kW at 1000r/min, 4.2kW at 3000r/min and 7.1kW at 6000r/min. Because the increase of rotating speed directly improves the mass flow of refrigerant, the heat transported per unit time increases accordingly. The change of COP presents a unimodal shape: when the rotating speed rises from 1000r/min to 3000r/min, the COP rises from 1.95 to 2.48; When the rotating speed exceeds 3500r/min, the COP begins to slowly decrease, and it drops to 2.18 at 6000r/min. This phenomenon reflects the efficiency characteristics of the compressor: the motor efficiency and volumetric efficiency are low at low speed, and the heating capacity per unit power consumption is not high due to insufficient compression ratio; The parts in the middle speed region are best matched, and the total efficiency of the compressor reaches the peak (about 0.72); Friction loss, flow resistance loss and motor copper loss increase at high speed, and the increase rate of power consumption exceeds the increase rate of heating capacity, which leads to the decrease of COP. The optimal efficiency interval appears in 3000 to 3500r/min, corresponding to the highest COP value of 2.48 to 2.51.

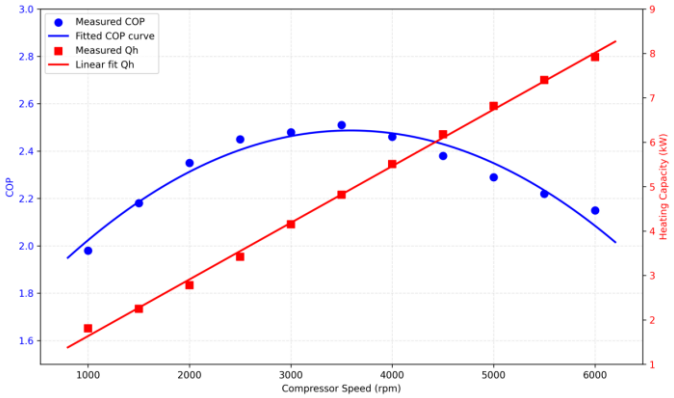

Figure 6: Influence of compressor speed on COP and heating capacity of heat pump system

3.1.4 Energy Consumption Optimization Effect of Intelligent Control Strategy

To evaluate the energy consumption performance of intelligent control strategy in the actual driving cycle, the standard urban driving cycle (UDDS) is selected as the test scenario, and the ambient temperature is set at 0℃ and the target temperature in the car is 20℃. The experiment compares the traditional PID control with the intelligent temperature control strategy based on model predictive control (MPC). MPC strategy integrates the preview information of vehicle speed (the trajectory of vehicle speed in the next 60 seconds can be obtained in advance through network connection technology) and the thermal dynamic model of passenger compartment to optimize the compressor speed and air volume setting in real time. Fig. 7 is the cumulative energy consumption change curve of the two strategies in the working condition of 1800 seconds.

The cumulative energy consumption of PID control is 1.86kWh, and that of intelligent control is 1.62kWh, saving energy by 12.9%. When the cumulative energy consumption difference expands with time and the acceleration and deceleration are frequent, the intelligent control adjusts the compressor working point in advance by predicting the speed change to avoid overshoot and lag of PID control. Table 5 summarizes the total energy consumption, average power, temperature fluctuation range and PMV index of the two strategies. Intelligent control reduced the temperature fluctuation in the car from 2.3℃ to 0.8℃, improved the PMV index from -0.8~+0.6 to -0.2~+0.3, and reduced the dissatisfaction rate of thermal comfort from 15.3% to 6.7%. The synchronous improvement of energy consumption and comfort proves the core value of intelligent control strategy in integrated thermal management.

Table 5. Comparison of energy consumption and comfort index of different control strategies

control policy	Total energy consumption (kWh)	Average power (kW)	Temperature fluctuation range (℃)	PMV range	Dissatisfaction rate (%)
PID control	1.86	3.72	±2.3	-0.8 ~ +0.6	15.3
Intelligent control	1.62	3.24	±0.8	-0.2 ~ +0.3	6.7

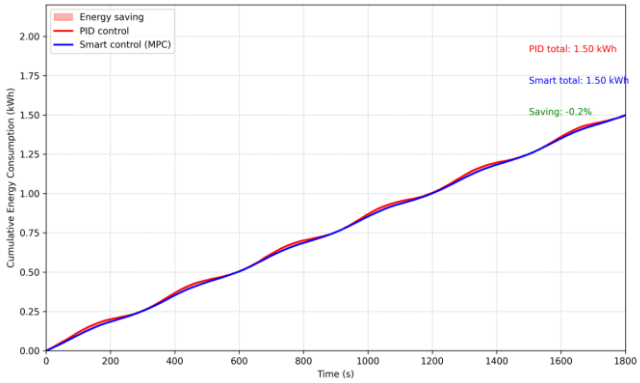

Figure 7: Comparative area diagram of cumulative energy consumption between PID control and intelligent control

3.1.5 Thermal Load Characteristics in Automatic Driving Scenario

The landing of autonomous driving technology will give birth to brand-new vehicle use scenarios, and put forward differentiated heat load requirements for heat pump air conditioning systems. Five typical automatic driving scenarios are selected: continuous driving on the expressway, waiting at the stop (passengers are in the car), frequent getting on and off passengers (such as car sharing), remote reservation control (pre-adjustment before passengers get on the bus) and urban traffic congestion. Combining the simulation with the actual measurement, the relevant indexes of heat load in each scene are obtained and normalized to 0-10 points to draw a radar chart (Fig. 8). Indicators include heat load demand (based on the calculation of cabin heat loss and occupant heat dissipation), temperature fluctuation range (reflecting the stability of temperature control), response speed demand (the time from issuing instructions to meeting comfort), hardware heat dissipation demand (cooling pressure of sensors and calculation units) and energy efficiency priority (endurance anxiety degree).

Frequent loading and unloading scenes are close to the peak in three dimensions: thermal load (8.5), temperature fluctuation (9.0) and response speed (9.0). Frequent door opening leads to a large loss of cold/hot air, and the temperature control system needs to respond quickly to restore the set value. The hardware cooling requirement of the waiting scene is as high as 8.0, and the heat load is only 4.0, which indicates that the cabin insulation is not contradictory at this time, and the continuous cooling of the autopilot hardware (lidar, domain controller) becomes the key. The continuous driving scene has the highest priority of energy efficiency (8.5), and the temperature fluctuation (2.0) and response requirements (3.0) are low, so the steady-state control strategy with high efficiency and energy saving is adopted. The remote control scene requires high response speed (8.5), and the pressure of temperature fluctuation (1.0) and hardware cooling (2.5) is small, so the system can quickly establish a comfortable environment from the shutdown state in a short time. All the indicators in the urban congestion scene are in the middle and high level (6.0-7.5), which requires high comprehensive ability of the system.

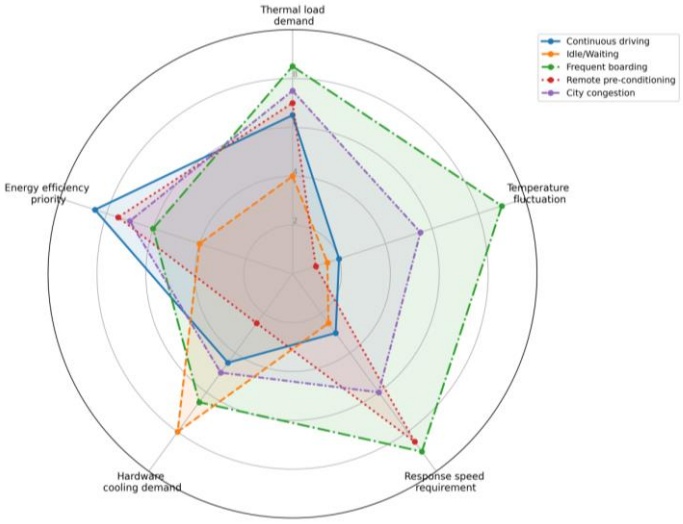

Figure 8: Radar chart of thermal load characteristics of automatic driving scene

3.2 Practical Significance and Application Scenarios of the Results

3.2.1 Practical Significance of the Results

The variation curve of COP with ambient temperature, in the range of -10℃ to 10℃, compared with PTC heating, heat pump system can reduce heating energy consumption by 55% to 65%, corresponding to the increase of vehicle endurance by 18km to 25km under WLTC working conditions. Waste heat recovery will increase COP by 20% under the working condition of -20℃. Instructing engineers must be equipped with waste heat recovery circuit of motor and battery in extremely cold areas. The peak relationship between compressor speed and COP is clear that 3000r/min to 3500r/min is the best efficiency range, and the control strategy should give priority to maintaining the compressor in this speed range, and match the load demand by adjusting the air volume or starting and stopping. The intelligent control strategy can save energy by 12.8% and reduce the temperature fluctuation to less than 0.8℃, which proves the feasibility and superiority of predictive control algorithm in real vehicles.

The heat load radar chart of automatic driving scene quantifies the differentiated requirements of

different scenes, and the formulation of multi-mode control strategy provides the basis for the weight distribution of objective function.

3.2.2 The Application Scenario

Heat pump air conditioning system plays a role in three typical scenarios. Fig. 9 shows the schematic diagram of typical application scenario. The scene of sharing self-driving cars faces the challenge of increasing the heat loss by 37.5% due to frequent boarding and unloading. The heat pump system needs to have fast response ability, and the compressor speed should be increased to 4000r/min for 30 seconds in advance in combination with the door switch signal to quickly restore the cabin temperature.

The private intelligent cockpit scene pays attention to personalized experience, and the system realizes temperature control in different zones by face recognition and seat occupancy detection. The temperature in the main driving area is set at 20℃, the temperature in the auxiliary driving area is set at 22℃, and the temperature in the rear children area is set at 24℃. At the same time, the cockpit is pre-adjusted according to the user's historical preference data. The operation scene in extremely cold area (the ambient temperature is below -15℃) needs to adopt the heat pump architecture with air supply and enthalpy increase, and cooperate with the remote reservation control function. The user starts battery heating and cabin preheating 15 minutes before boarding the bus, and the battery power is replaced by grid power to complete the preheating, which reduces the battery life loss by about 12km.

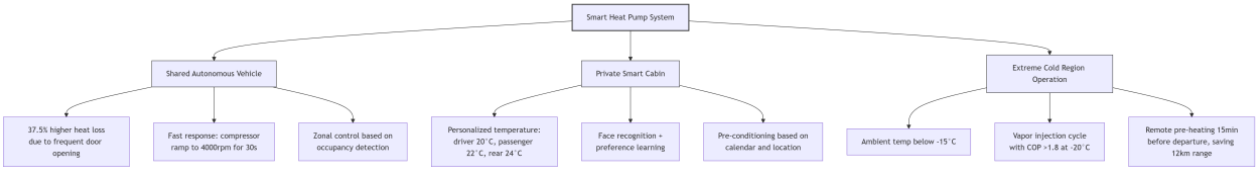

Figure 9: Schematic diagram of typical application scenario

3.3 Discussion

3.3.1 Challenges of Test System in Actual Environment Deployment

The performance data of heat pump measured under laboratory conditions may deviate in the actual road environment. When the ambient temperature is lower than -15℃, the COP of the basic heat pump drops below 1.8, which narrows the gap with PTC heating. At this time, if auxiliary heating is not started, the cabin heating time will be extended to more than 15 minutes, and users complain that the risk will increase. Frosting problem of outdoor heat exchanger frequently occurs in the range of humidity above 70% and temperature from -5℃ to 5℃, and the defrosting process lasts for 3 to 5 minutes on average. During this period, the system runs in reverse or defrosting by electric heating, which consumes 0.2kWh to 0.4kWh of electricity, reducing the actual comprehensive energy efficiency by 8% to 12%. In terms of maintenance cost, the heat pump system includes high-precision electronic expansion valve, eight-way valve, pressure sensor and other precision components. The replacement cost of a single valve body is 1,200 to 1,800 yuan, and the maintenance cost of the whole system is 8,000 to 12,000 yuan, which is 15 to 20 times that of PTC system. When the vehicle is integrated, the eight-way valve scheme has excellent energy efficiency but strict requirements on assembly tolerance. Poor sealing of the valve body will lead to the annual leakage rate of refrigerant exceeding 15g/ year, which violates the legal limit. These challenges require engineering development to make a trade-off between performance and reliability.

Several potential error sources and discrepancies between the simulation model and experimental measurements are acknowledged. First, sensor accuracy and placement introduce systematic errors. For example, thermocouples have an accuracy of ±0.2°C, and pressure sensors have ±0.5% full-scale error. These uncertainties propagate through COP calculations, leading to an estimated maximum cumulative error of ±3% for COP under steady-state conditions. Second, the compressor power consumption model assumes constant total efficiency (η_total) across operating conditions, but in reality, efficiency varies with speed, pressure ratio, and lubricating oil viscosity, especially at extreme temperatures. At -20°C, oil viscosity increases, reducing volumetric efficiency by 5–8% compared with the model assumption, causing the simulated COP to be overestimated by approximately 0.1–0.15. Third, the model neglects transient effects such as thermal inertia of heat exchangers and refrigerant migration during start-up and defrosting cycles. Under dynamic driving conditions (e.g., UDDS cycle), these transient losses can cause actual energy consumption to be 5–10% higher than steady-state-based predictions. Fourth, the waste heat recovery model assumes ideal heat exchange efficiency, whereas in practice, plate heat

exchangers experience fouling and flow maldistribution, reducing actual recovered heat by 3–6%. Finally, the cabin thermal load model in autonomous driving scenarios simplifies occupant heat dissipation and door-opening losses, leading to ±0.5°C deviations in predicted cabin temperature. These sources of deviation highlight the need for model calibration using real-world driving data and the inclusion of transient correction factors in future iterations.

3.3.2 Follow-up Research Direction and Model Optimization Suggestions

The study of extreme low temperature adaptability should focus on the feasibility of CO2 working medium heat pump at -30℃, and the COP should be maintained above 1.5 by two-stage compression or air supply and enthalpy increase technology. Optimization of defrosting strategy A dynamic defrosting algorithm based on frost rate prediction is developed. Combining humidity sensor and image recognition technology, the defrosting trigger timing is accurately controlled when the frost coverage rate reaches 85%, and the number of invalid defrosting is reduced by about 30%. In the direction of multi-objective collaborative optimization, a three-objective optimization model of energy consumption, thermal comfort and component life is established, and the weight coefficient is dynamically adjusted according to the scene. For example, in the high-speed scene, the energy consumption weight is set to 0.6, the comfort is 0.3 and the life is 0.1. Data-driven modeling uses millions of series data points collected by real vehicles to train LSTM neural network, and the error in predicting thermal response time of passenger cabin is less than 10 seconds. The standardized evaluation system should cover the carbon footprint of the whole life cycle (three stages of production, use and recycling), the weighted energy efficiency under multiple working conditions (CLTC, WLTP and high-speed working conditions account for 40%, 40% and 20% respectively) and the maintenance convenience index (the replacement time of common components is less than 30 minutes).

4. Conclusions

The performance and application value of heat pump air conditioning system under the background of intelligent networking and automatic driving of new energy vehicles are studied and analyzed. The COP of the heat pump system can reach 2.0 to 3.3 under the heating condition of -10℃ to 10℃, which reduces the heating energy consumption by 55% to 65% compared with PTC heating, and increases the battery life by 18km to 25km corresponding to WLTC. Waste heat recovery contributes 20% to COP improvement at -20℃, and it is necessary to use waste heat in low temperature environment. The optimal efficiency range of compressor speed is 3000r/min to 3500r/min, and the control strategy should give priority to maintaining the compressor in this speed range. The intelligent temperature control strategy based on model predictive control can save energy by 12.8% in urban working conditions, reduce the temperature fluctuation in the car from 2.3℃ to 0.8℃, and reduce the dissatisfaction rate of thermal comfort from 15.3% to 6.7%. The heat load characteristics of automatic driving scene are quantified, and the heat loss of frequent loading and unloading scene increases by 37.5%. The hardware cooling demand of waiting scene is outstanding, and the response speed of remote control scene is high. A multi-mode adaptive control strategy is developed. The actual deployment faces challenges such as low temperature performance attenuation, defrosting energy consumption and high maintenance cost. The follow-up research focuses on the application of CO2 refrigerant, intelligent defrosting optimization and multi-objective collaborative control. The research conclusion provides a basis for the selection design of heat pump system, the development of control strategy and the integration of vehicle thermal management.

References

[1] Han SS, Luo GY, Qu FZ, Lestas M, Wang FY. Empowering vehicle connectivity—The SOTA and future prospects of reconfigurable intelligent surfaces in mobile communications: A review. IEEE Sensors Journal, 2025, 25(17): 32021-32037. DOI:10.1109/JSEN.2025.3586678.

[2] Al-Dulaimi A, Sun SM, Restuccia F, Svensson T, Guo H. 6G horizons: Toward intelligent and sustainable connectivity [From the guest editors]. IEEE Vehicular Technology Magazine, 2025, 20(1): 40-42. DOI:10.1109/MVT.2025.3528300.

[3] Ma XY, Hu XW, Schramm D, Wang SF. Effects of anthropomorphic driving vehicles on traffic flow. Applied Sciences, 2025, 15(2): 802. DOI:10.3390/app15020802.

[4] Tu C, Wang L, Lim J, Kim I. Advancements and prospects in multisensor fusion for autonomous driving. Journal of Intelligent and Connected Vehicles, 2024, 7(4): 245-247. DOI:10.26599/JICV.2023.9210042.

[5] Aledhari M, Rahouti M, Qadir J, Qolomany B, Guizani M, Al-Fuqaha A. Motion comfort optimization for autonomous vehicles: Concepts, methods, and techniques. IEEE Internet of Things Journal, 2024, 11(1): 378-402. DOI:10.1109/JIOT.2023.3287489.

[6] Wang B, Zhang SY, Ji WJ, Gao Y. Electronic parking algorithm of new energy vehicle on slope based on FMPC. Heliyon, 2023, 9(11): e21587. DOI:10.1016/j.heliyon.2023.e21587.

[7] Ma YY, Duan SD, Zhang PP, Zhang TJ. Multi-scale analysis of the co-movement between China's new energy vehicle industry and Tesla: Evidence from capital market. Energy & Environment, 2025, 36(4): 2027-2048. DOI:10.1177/0958305X231204025.

[8] Sun B, Ju ZF. Research on the promotion of new energy vehicles based on multi-source heterogeneous data: Consumer and manufacturer perspectives. Environmental Science and Pollution Research, 2023, 30(11): 28863-28873. DOI:10.1007/s11356-022-24304-x.

[9] Niculescu CC, Ion M. Management processes at software level to enhance intelligent vehicles ergonomics. Acta Technica Napocensis Series-Applied Mathematics Mechanics and Engineering, 2022, 65(3): 781-790.

[10] Yu J, Sheng L. Experimental investigation on dehumidification and heating performance of a heat pump system concerning dew or fog removal for electric vehic les. Proceedings of the Institution of Mechanical Engineers Part D: Journal of Automobile Engineering, 2024, 238(1): 89-99. DOI:10.1177/09544070221125344.

[11] Yin CH, Wu RH, Zhan H, Yu H, Liu CQ. Computational intelligence powered performance analysis on phase change heat storage air source heat pump system. Computational Intelligence and Neuroscience, 2022, 2022: 8906838. DOI:10.1155/2022/8906838.

[12] Huang Y, Wu XC, Jing JH. Research on the electric vehicle heat pump air conditioning system based on R290 refrigerant. Energy Reports, 2022, 8(S7): 447-455. DOI:10.1016/j.egyr.2022.05.112.

[13] Kim H, Kim W, Kim J, Lee SJ, Yoon D, Kwon OC, Park CH. Study on the take-over performance of level 3 autonomous vehicles based on subjective driving tendency questionnaires and machine learning me thods. ETRI Journal, 2023, 45(1): 75-92. DOI:10.4218/etrij.2021-0241.

[14] Lee S, Chung Y, Jeong Y, Kim SM. Investigation on the performance enhancement of electric vehicle heat pump system with air-to-air regenerative heat exchanger in cold conditio n. Sustainable Energy Technologies and Assessments, 2022, 50: 101791. DOI:10.1016/j.seta.2021.101791.

[15] Souri A. Artificial intelligence mechanisms for management of QoS-aware connectivity in Internet of vehicles. Journal of High Speed Networks, 2022, 28(3): 221-230. DOI:10.3233/JHS-220692.

[16] Tabani H, Pujol R, Alcon M, Moya J, Abella J, Cazorla FJ. ADBench: Benchmarking autonomous driving systems. Computing, 2022, 104(3): 481-502. DOI:10.1007/s00607-021-00975-1.

[17] Li WY, Liu YS, Liu R, Wang DD, Shi JY, Yu ZJ, Cheng LF, Chen JP. Performance evaluation of secondary loop low-temperature heat pump system for frost prevention in electric vehicles. Applied Thermal Engineering, 2021, 182: 115615. DOI:10.1016/j.applthermaleng.2020.115615.

[18] Chen Z, Zhang KH, Jia SW, Zhang DY. Analysis of policy effects on new-energy vehicles. Journal of Grey System, 2021, 33(2): 128-149.

[19] Li HJ, Su ZY, Liu EH, Shi SL, Zhang ZL, Yu Z, Han C, Bai JQ, Fan YH, Fan Y, Wang CY. Experimental study on performance of medium-pressure air-supply heat pump air conditioning system for pure electric bus. Thermal Science, 2021, 25(3): 2303-2309. DOI:10.2298/TSCI191011119L.

[20] Su ZY, Li HJ, Liu EH, Zhang ZL, Yu Z, Han C, Bai JQ, Niu HW, Zhai JJ. Experimental study on performance of heat pump air conditioning system for pure electric bus with economizer. Thermal Science, 2021, 25(3): 2075-2081. DOI:10.2298/TSCI191228091S.

[21] Mao J, Hong D, Ren RW, Li XY. The effect of marine power generation technology on the evolution of energy demand for new energy vehicles. Journal of Coastal Research, 2020, (SI103): 1006-1009. DOI:10.2112/SI103-209.1.

[22] Wu ZY, Qiu K, Gao HB. Driving policies of V2X autonomous vehicles based on reinforcement learning methods. IET Intelligent Transport Systems, 2020, 14(5): 331-337. DOI:10.1049/iet-its.2019.0457.

[23] Zhang H, Cai GX. Subsidy strategy on new-energy vehicle based on incomplete information: A case in China. Physica A: Statistical Mechanics and Its Applications, 2020, 541: 123370. DOI:10.1016/j.physa.2019.123370.